

# A Metric for Selecting Waveforms of Multi-User Wideband Active Sonars

Cheng Chi, Hari Vishnu and Mandar Chitre

Acoustic Research Laboratory, Tropical Marine Science Institute, National University of Singapore, Singapore  
tmschic@nus.edu.sg; hari@arl.nus.edu.sg; mandar@arl.nus.edu.sg

**Abstract**—This paper focuses on selection of suitable waveforms for multi-user wideband active sonars. A metric for selecting waveforms for multi-user sonar operation is proposed, namely the multi-user sonar average lobe level. The proposed metric considers both the sidelobe levels of the auto-ambiguity functions and the lobe levels of the cross-ambiguity functions of the waveforms. Our simulations show that the proposed metric can be an accurate indicator of the detection performance of different waveforms in the case of multi-user sonars. This accuracy would not be possible by using only the auto or cross ambiguity functions in isolation for prediction. The proposed metric can help select better waveforms for multi-user sonars.

**Keywords**—Cross ambiguity function, multi-user sonar, metrics, wideband ambiguity function, waveform selection

## I. INTRODUCTION

In some underwater monitoring scenarios, a single operating active sonar may not be able to yield a sufficient range and coverage area required for the application. In such scenarios, multiple active sonar systems operating simultaneously can solve the problem of coverage area [1]. The bandwidth available may be limited in such systems, especially if operating a low frequency active sonar setup, hence the sonar users may be required to operate in the same bandwidth. Also, it may not be possible to synchronize and time-slice their pings. The challenge in operating such a system is that the mutual interference between multiple sonar users will deteriorate the detection performance of each user [2]-[5].

Generally, the wideband auto-ambiguity function (AAF) is the tool employed to analyze the performance of a single waveform used in a single sonar setup [5], [6]. However, waveforms that exhibit a good performance in the case of single operating sonar, do not necessarily perform well in the case of multiple operating users. Some works have looked at analyzing the effect of inter-sonar interference in a multi-user setup using the cross-ambiguity function (CAF) as well [3], [4], but this alone is not indicative of the performance of the system in an application scenario. Thus, the relationship between the ambiguity functions of the waveforms and how

they could be indicative of their operating performance, is not yet established.

In this paper, we study the relationship between the ambiguity function metrics and the operating performance of a multi-user sonar setup, in terms of its joint probability of detection (PD). We propose a metric of multi-user sonar performance named the multi-user sonar average lobe level. This considers a combination of both the AAF and CAF. We show that the proposed multi-user sonar average lobe level is a good metric for selecting waveforms of multi-user sonars.

Based on [7]-[10], the waveforms used in sonar and radar can be broadly classified into three families: phase-coded, frequency hop (FH) and frequency-modulated. Thus, in our paper, three waveforms representing each of these families respectively are chosen as the candidates for comparison for multi-user sonars: Gold codes [11], hyperbolic FH [4], and orthogonal linear frequency modulated (LFM) [8], [10]. In Section V, simulation results are presented to evaluate the detection performance and verify the validity of the proposed metric.

This paper is organized as follows. In Section II, we briefly introduce the wideband AAF and CAF. In section III, we discuss the metrics for multi-user sonars and propose our metric. Three typical waveforms for multi-user sonars are presented and discussed in Section IV. Section V presents the simulation results to verify the proposed metric. Finally, conclusions are given in Section VI.

## II. WIDEBAND AMBIGUITY FUNCTION

Active sonar operation may often involve transmission of wideband signals, [2], [7], [14]. In this scenario, the narrowband ambiguity function that is popular in the radar literature, cannot be used for analyzing the properties of the waveforms. The wideband ambiguity function should be employed to analyze the waveforms in this case. This paper discusses multi-user sonars. Thus, the definition of the wideband ambiguity functions for the waveforms must

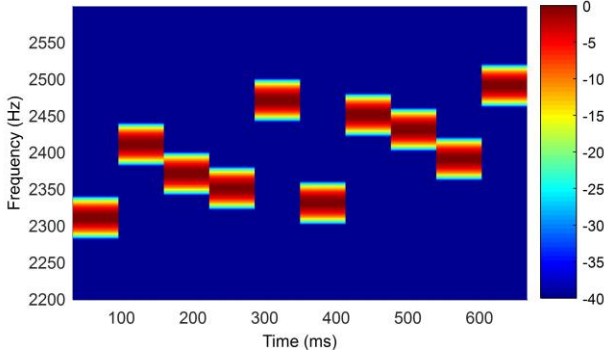


Fig. 1. Spectrogram of the frequency hop waveform.

describe the delay-Doppler correlation for more than just one waveform, to account for the cross-talks between sonars.  $K$  waveforms for  $K$  simultaneous sonar users are considered in this paper, where  $K > 1$ .

The wideband ambiguity function can be defined as [5], [6]

$$\chi_{k,m}(\lambda, \tau) = \sqrt{\lambda} \int_{-\infty}^{\infty} s_k(t) s_m^*(\lambda(t + \tau)) dt, \quad (1)$$

where  $s_k(t)$  and  $s_m(t)$  are the energy normalized analytic signals transmitted by the  $k^{\text{th}}$  user and the  $m^{\text{th}}$  user,  $\tau$  is the time delay, and  $\lambda$  is the compression factor associated with Doppler due to a radial velocity  $v$  of the target.  $\lambda$  is given by

$$\lambda = \frac{c - v}{c + v}, \quad (2)$$

where  $c$  is the sound speed. The two analytic signals  $s_k(t)$  and  $s_m(t)$  can be expressed as [5]

$$\begin{cases} s_k(t) = u_k(t) e^{j\omega_0 t} \\ s_m(t) = u_m(t) e^{j\omega_0 t} \end{cases}, \quad (3)$$

where  $\omega_0$  is the spectral centroid,  $u_k(t)$  and  $u_m(t)$  are the complex envelopes of  $s_k(t)$  and  $s_m(t)$  respectively.

When  $k = m$ , (1) represents the wideband AAF, which is indicative of each sonar's individual performance when used in isolation. When  $k \neq m$ , (1) represents the wideband CAF, which indicates the cross-talk between the sonars. For designing a single-user sonar, we only need to consider the wideband AAF. However, for designing multi-user sonars, both the wideband AAF and CAF should be considered.

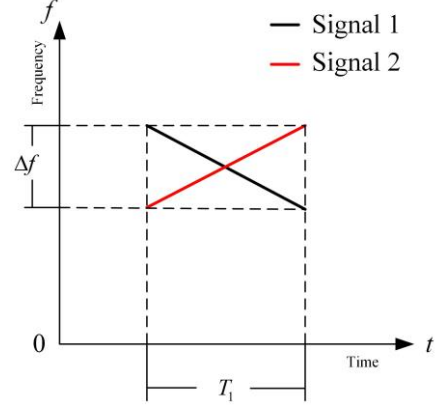


Fig. 2. Schematic diagram of the orthogonal LFM waveforms for 2-user sonar.

### III. PROPOSED METRICS

One strategy to select transmit waveforms for multi-user sonar operation is to test their performances via Monte Carlo simulations, which can often be computationally intensive. It would be easier to select these waveforms if a simple indicative metric is available for this purpose. This would alleviate the need to undertake computationally complex Monte Carlo simulations for this purpose each time waveform selection is required, and could also enable dynamic waveform selection if needed. The published literature [3], [4], [11] on multi-user sonars considers selection metrics that focus on evaluating and minimizing the interferences among different users. However, the limitation of this approach is that it only helps alleviate the cross-talk between sonars, but does not maximize the overall performance of the multi-user system. In fact, if the sidelobe levels of the AAF are high, the overall performance of the multi-user system would still be poor, even if the mutual interferences are low.

We propose that a selection metric that encapsulates the overall performance of a multi-user sonar system must consider an aggregate of each sonar system's individual performance, and their interference with each other. We first define an aggregate metric of a single ambiguity function named as average lobe level (ALL), which is expressed as

$$L(k, m) = \frac{1}{A_{k,m}} \iint_{S_{k,m}} |\chi_{k,m}(\lambda, \tau)| d\tau d\lambda, \quad (4)$$

where  $S_{k,m}$  indicates the lobe region of the delay-Doppler plane  $\lambda$ - $\tau$  considered, and  $A_{k,m}$  is the area of this region. This yields the 1-norm of the lobe levels within the region  $S_{k,m}$ .

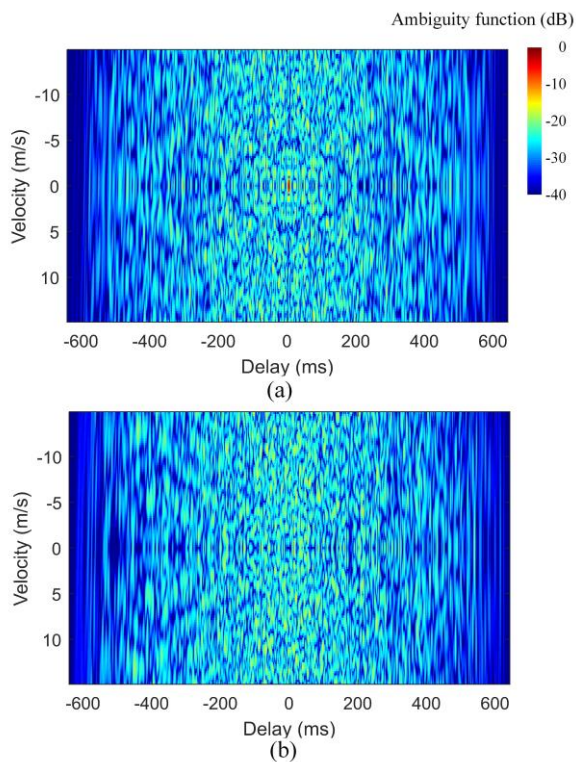


Fig. 3. Peak-normalized wideband (a) AAF and (b) CAF of the Gold sequences selected.

We now propose a metric for the selection of waveforms which is the sum of ALL aggregates of the AAF and CAF. The proposed metric, named multi-user sonar average lobe level (MSALL), is defined as

$$L_{MS} = \frac{1}{K^2} \sum_{k=1}^K \sum_{m=1}^K L(k, m). \quad (5)$$

From (5), it should be noted that the proposed metric MSALL jointly considers the lobe levels of the AAF and CAF. Here, it should also be emphasized that for the AAF, we consider only the sidelobes (i.e., the region away from the mainlobe), but for the CAF, the whole delay-Doppler response within the range/Doppler limits of interest needs to be considered. Hence, the term ‘lobe’ is used more frequently in this paper to generically refer to both these lobe levels. The MSALL is an indicator of how poor the detection performance of the system is expected to be, i.e., larger the MSALL, poorer the performance.

#### IV. TYPICAL WAVEFORMS FOR MULTI-USER SONARS

Based on the literature [7]-[10], three families of waveforms are commonly used in active sonar: phase-coded,

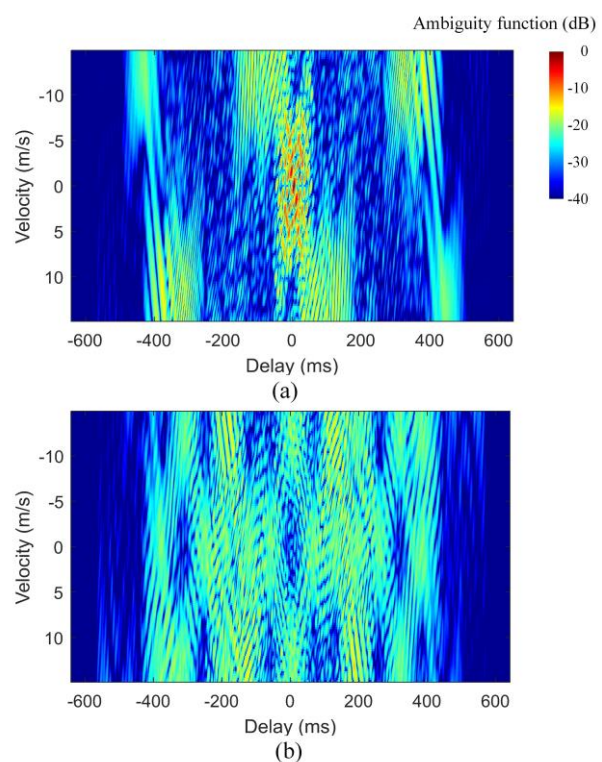


Fig. 4. Peak-normalized wideband (a) AAF and (b) CAF of the hyperbolic frequency hop codes selected.

frequency hop, and LFM. In the following, we discuss three representative waveforms from each of these families, and use them in a comparative study to verify our proposed metric.

The phase-coded waveforms can be expressed in baseband as [12]

$$s_{PC}(t) = \sum_{n=1}^N \text{rect}\left(\frac{t - nT_1}{T_1}\right) e^{j\varphi_n}, \quad (6)$$

where  $N$  is the code length,  $\text{rect}(\cdot)$  is the rectangular window function,  $T_1$  is the duration of each code element, and  $\varphi_n$  is the phase of the  $n^{\text{th}}$  code element. Among binary phase-coded signals, Gold and Kasami codes have received some attention for several multi-user applications. The reference [11] demonstrates that Gold codes perform well for multi-user applications. Thus, we choose Gold codes as candidates for multi-user sonar as a representative waveform of binary phase coded signals.

The FH waveform [13] can be expressed in baseband as

$$s_{FH}(t) = \sum_{q=0}^{Q-1} \text{rect}\left(\frac{t - q\Delta t}{\Delta t}\right) e^{j2\pi c_q \Delta t}, \quad (7)$$

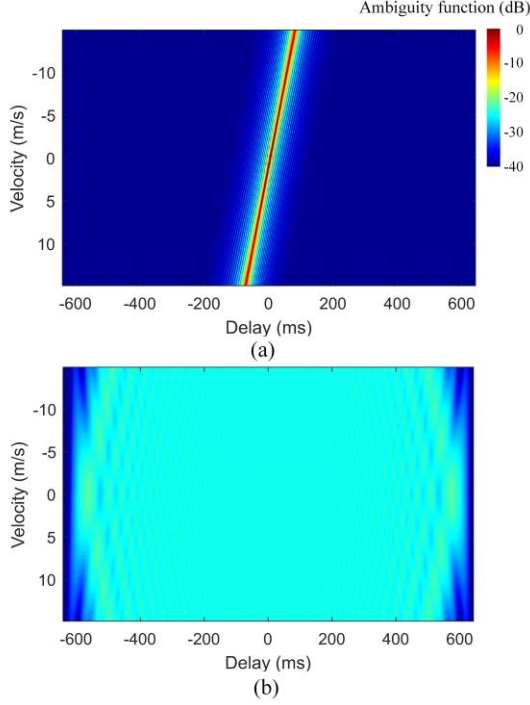


Fig. 5. Peak-normalized wideband (a) AAF and (b) CAF of the orthogonal LFM waveforms selected.

where  $c_q$  is the  $q^{\text{th}}$  element of the frequency hop codes,  $Q$  is the length of the code,  $\Delta t$  is the duration of one code element, and  $\Delta f$  is the sub-bandwidth of each FH bin, given by

$$\Delta f = B / Q, \quad (8)$$

where  $B$  is the bandwidth of the transmitted waveform. The reference [4] suggests that the hyperbolic FH codes can achieve nearly ideal characteristics for multi-user applications. The authors claim that for multi-user sonar, these waveforms are a good choice for operation amongst possible FH waveforms. Hence we choose the hyperbolic FH code as a representative of the FH class of waveforms. Fig. 1 shows a spectrogram of an example hyperbolic FH code.

The waveform of a LFM [10] is expressed in baseband as

$$s_{\text{LFM}}(t) = e^{j2\pi\left(\frac{\mu}{2}t^2\right)}, \quad -T_0/2 \leq t \leq T_0/2 \quad (9)$$

where  $\mu$  is the rate of frequency change and  $T_0$  is the waveform duration. If there are only two users, LFM waveforms can be employed in 2 configurations, one with an up-sweep across the bandwidth, and one with a down-sweep as shown in the schematic in Fig. 2. We use two LFM waveforms: one with a

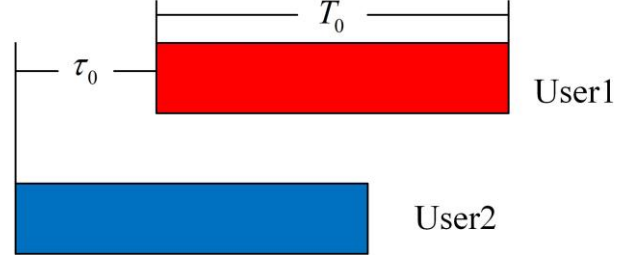


Fig. 6. Schematic diagram of signal transmissions in the simulation setup.  $\tau_0$  is the random delay distributed as per a uniform distribution, and  $-T_0 < \tau_0 < T_0$ .

TABLE I. DIFFERENT METRICS OF THE THREE WAVEFORMS

Waveform	Average lobe level (CAF, dB)	Average lobe level (AAF, dB)	Multi-user sonar average lobe level (dB)
Gold	-27.94	-28.90	-28.40
FH	-26.39	-33.90	-29.34
LFM	-24.34	-50.46	-29.95

(Gold: Gold code; FH: hyperbolic frequency hop)

positive value of  $\mu$  and one with a negative value, which are nearly orthogonal with respect to each other.

Figs. 3-5 show the AAFs and CAFs of the three selected waveforms. All the waveforms are designed to be of the same duration of 635 ms. The operating bandwidth is 200 Hz and central frequency is 2.4 kHz. We consider targets within the velocity range -15 m/s to 15 m/s, hence this Doppler range is considered in all the ambiguity functions. The hyperbolic FH waveforms are designed to use a code with 10 elements. The Gold codes are designed to have a 127-digit long code.

We now define the ambiguity function regions over which the metric is computed. When  $k \neq m$ , the CAF represents the cross-talk aspect of the multi-user sonar performance. For a particular sonar user, cross-talk from another user occurring anywhere within the delay/Doppler range of interest would influence its sonar performance. Thus, for the CAF, the lobe region considered in the metric is the whole Doppler-delay plane of interest.

When  $k = m$ , the lobe regions of the AAF should be divided into two regions: sidelobe and mainlobe. The energy in the mainlobe indicates the delay-Doppler regime that is detected during matched filtering, whereas energy in the sidelobe is likely to cause false alarms and is hence adverse to detection. Thus, we only consider the sidelobe region of the AAF in the

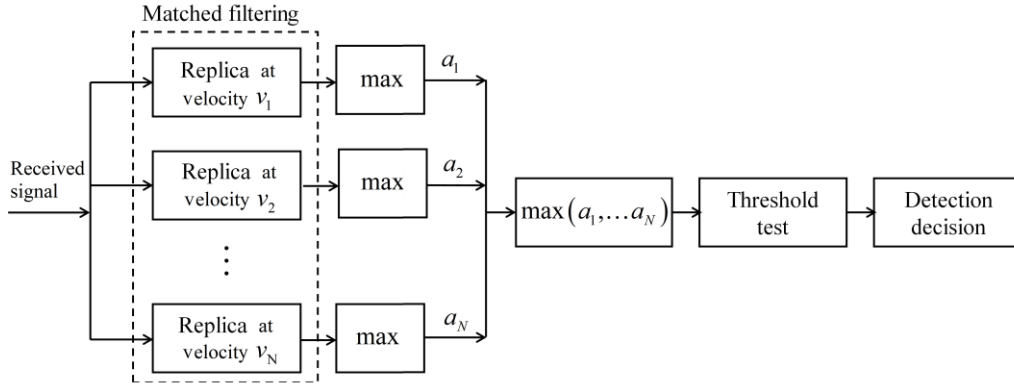


Fig. 7. Schematic of the detector used in simulations to test performance. The received signal is matched-filtered against several Doppler-shifted replicas at velocity channels  $v_1, v_2, \dots, v_N$ . The maximum of the matched-filter output at the  $i^{\text{th}}$  channel is represented by  $a_i$ , and the test statistic is computed as the maximum of all the  $a_i$ s.

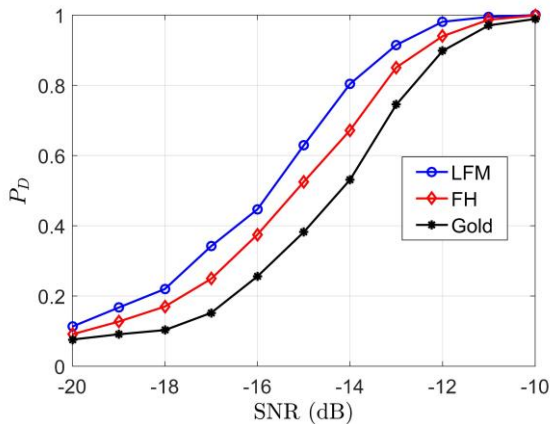


Fig. 8. Variation of probability of detection of the three waveform groups considered in multi-user sonar setup, against received SNR.

metric. From Fig. 5, we see that the mainlobe of the LFM has a ridge-like slanted structure. At -15 m/s, the main lobe falls off to -20 dB at 70 ms delay. We define the mainlobe region as lying within this -20 dB boundary for the LFM. The sidelobe region is defined as where the delay magnitude exceeds 70ms, and the velocity magnitude is within 15 m/s. For consistency of comparison, we use this definition for all the three waveforms.

Table I presents the different metrics for the three waveforms. The simulations in Section V will show that the performance comparison of the three waveforms matches the trends of the MSALL metric proposed here.

## V. SIMULATION

In our current simulation, two users are considered. The setup of signal transmissions by the two users in our simulations, is shown in Fig. 6. It is assumed that the users do not have time-synchronization with each other, and the

transmitting delay between the two users is uniform randomly distributed. A basic binary-hypothesis testing is used to evaluate detection performance based on Neyman-Pearson criteria. A matched filter detector is employed at the receivers. A schematic of the detector employed [7], [8] is shown in Fig. 7. Our detection test statistic is a search for the largest peak across all delays and Doppler channels of interest.

For the simulation scenario, we consider a shallow water acoustic channel with time-varying multipath. The single target is assumed to be at a range of 5 km. We incorporate channel variability due to multipath encountered in shallow water channels, using a model that incorporates fluctuations caused by time-varying multipath and fading [15]. The received echoes at the sonar are modeled based on a two-way propagation through the channel from transmitter to the target and back. The parameters of the channel used in simulations are as follows. The speed of sound in water is set at  $c = 1540$  m/s, speed of sound in sediment is set at 1650 m/s, channel depth is set at 20 m and source, receiver and target depths are set at 10 m. Attenuation factor in sediment is set at 0.1, density of sound in sediment is set as  $1200 \text{ kg/m}^3$ . The received signals are assumed to be contaminated with white Gaussian noise.

The variation of the probabilities of detection of the three waveforms against the signal-to-noise (SNR) of the received signal, are shown in Fig. 8. It can be found that in terms of detection performance, the orthogonal LFM waveforms are better than the hyperbolic FH waveforms by 0.7 dB at  $PD = 0.8$ . The FH waveforms are in turn better than the Gold code by 0.8 dB at  $PD = 0.8$ .

Table I shows three metrics: the ALL of the AAF and CAF, and the proposed MSALL metric. From Table I, it can be seen

that trends of the proposed MSALL match the trend of the PD results well. This shows that the proposed metric is a good indicator of the relative detection performance of these waveforms.

## VI. CONCLUSION

In this paper, we propose a metric for selecting waveforms for use in multi-user sonar. We demonstrate that when used in isolation, the ALL of auto or cross ambiguity functions are not suitable metrics to evaluate a transmit waveform's performance. The proposed metric MSALL combines the average lobe level of auto and cross ambiguity functions. We show that this metric is an effective indicator of the relative detection performance of these waveforms as evaluated in our simulations. The proposed metric can be utilized for the selection or design of better waveforms for multi-user sonars, without the need to undertake extensive Monte Carlo simulations.

Furthermore, our simulations compare the detection performance in terms of joint PD, of three representative waveforms from three families of transmit signals. When there are only two sonar users, the orthogonal LFM pair are an effective candidate for use. However, the orthogonal LFM cannot be scaled for more than two users in an effective and straightforward way. Thus, when considering more than two users, the hyperbolic frequency hop waveforms are a good choice as candidate waveforms for multi-user sonar operation.

## REFERENCES

- [1] R. Been, S. Jespers, S. Coraluppi, C. Carthel, C. Strode, and A. Vermeij, "Multistatic sonar: a road to a maritime network enabled capability," *Proceedings of Undersea Defence Technology Europe*, 2007.
- [2] R. C. Trider, "Signal investigation for low frequency active (LFA) sonar," *Defence Research and Development Canada, Contract report 2015-C05*, Mar. 2012.
- [3] S. Pecknold, "Ambiguity and cross-ambiguity properties of some reverberation suppressing waveforms," *Defence Research and Development Canada, TM 129*, 2002.
- [4] S. V. Maric and E. L. Titlebaum, "A class of frequency hop codes with nearly ideal characteristics for use in multiple-access spread-spectrum communications and radar and sonar systems," *IEEE Trans. Commun.*, vol. 40, no. 9, pp.1442-1447, Sep. 1992.
- [5] L. H. Sibul and E. L. Titlebaum, "Volume properties for the wideband ambiguity function," *IEEE Trans. Aerosp. Electron. Sys.*, vol. 17, no. 1, pp.83-87, Jan. 1981.
- [6] Z. Lin, "Wideband ambiguity function of broadband signals," *J. Acoust. Soc. Am.*, vol. 83, no. 6, pp. 2108-2116, Nov. 1988.
- [7] R. O. Nielsen, *Sonar Signal Processing*. Boston, MA, USA: Artech House, 1991, ch. 5.
- [8] M. A. Richards, *Fundamentals of Radar Signal Processing*. The McGraw-Hill Companies, Inc., 2005, ch. 4 and 6.
- [9] N. levanon and E. Mozeson, *Radar signals*. John Wiley & Sons, 2004.
- [10] B. R. Mahafza and A. Z. Eisherbeni, *MATLAB simulations for radar systems design*. Chapman and Hall/CRC, 2003, ch. 3.
- [11] D. V. Sarwate and . B. Pursley, "Crosscorrelation properties of pseudorandom and related sequences," *Proc. IEEE.*, vol. 68, no. 5, pp. 593-619, May. 1980.
- [12] C. Chi, Z. Li, and Q. Li, "Design of optimal multiple phase-coded signals for broadband acoustic Doppler current profiler," *IEEE J. Ocean. Eng.*, vol. 41, no. 2, pp. 302-317, Apr. 2016.
- [13] C. Y. Chen, and P. P. Vaidyanathan, "MIMO radar ambiguity properties and optimization using frequency-hopping waveforms," *IEEE Trans. Signal Process.*, vol. 56, no. 12, pp. 5926-5936, Dec. 2008.
- [14] Q. Li. *Digital sonar design in underwater acoustics: principles and applications*. Springer Science & Business Media., 2012.
- [15] M. Chitre, " A high-frequency warm shallow water acoustic communications channel model and measurements," *J. Acoust. Soc. Am.*, vol. 122, no. 5, pp. 2580-2586, Nov. 2007.